DSF-38-2001, astro-ph/0112384

Radiative corrections to neutrino energy loss rate in stellar interiors

S. Esposito, G. Mangano, G. Miele, I. Picardi, and O. Pisanti

Dipartimento di Scienze Fisiche, Università di Napoli Federico II and INFN, Sezione di Napoli, Complesso Universitario di Monte S. Angelo, Via Cintia, I-80126 Naples, Italy

Abstract

We consider radiative electromagnetic corrections, at order α, to the process $e^+e^- \to \nu\overline{\nu}$ at finite density and temperature. This process represents one of the main contributions to the cooling of stellar environments in the late stages of star evolution. We find that these corrections affect the energy loss rate by a factor $(-4 \div 1)\%$ with respect to the tree level estimate, in the temperature and density ranges where the neutrino pair production via e^+e^- annihilation is the most efficient cooling mechanism.

Key words: PACS 13.40.Ks, 95.30.Cq, 11.10.Wx

1 Introduction

The late stages of star evolution are strongly influenced by neutrino emission processes. After hydrogen burning, stars with small mass, of the order of the solar mass, evolves towards a white dwarf configuration. On the other hand more massive stars undergo several burning phases till the formation of a central iron core and the eventual triggering of the gravitational instability leading to the Supernova phenomenon. In both cases the cooling rate is largely dominated by neutrino production. For example, from the $^{12}C - ^{24}Mg$ burning phase, almost 100% of the energy flux is emitted via neutrino production, which leave the stellar system without any interaction because of their extremely large mean free path. A precise determination of neutrino emission rates is therefore a crucial issue in any careful study of the final branches of star evolutionary tracks. In particular, changing the cooling rates at the very

last stages of massive star evolution may sensibly affect the evolutionary time scale and the iron core configuration at the onset of the Supernova explosion, whose triggering mechanism is still lacking a full theoretical understanding [1].

The energy loss rate due to neutrino emission, hereafter denoted by Q, receives contribution from both weak nuclear reactions and purely leptonic processes. However for the rather large values of density and temperature which characterize the final stages of stellar evolution, the latter are largely dominant. They are mainly due to four possible interaction mechanisms:

i)	pair annihilation	$e^+ + e^- \rightarrow \nu + \overline{\nu}$
ii)	ν-photoproduction	$\gamma + e^\pm \rightarrow e^\pm + \nu + \overline{\nu}$
iii)	plasmon decay	$\gamma^* \rightarrow \nu + \overline{\nu}$
iv)	bremsstrahlung on nuclei	$e^\pm + Z \rightarrow e^\pm + Z + \nu + \overline{\nu}$

Actually each of these processes results to be the dominant contribution to Q in different regions in a density-temperature plane. For very large core temperatures, $T \gtrsim 10^9\,^\circ K$, and not too high values of density, pair annihilations are most efficient, while ν photoproduction gives the leading contribution for $10^8\,^\circ K \lesssim T \lesssim 10^9\,^\circ K$ and relatively low density, $\rho \lesssim 10^5$ g cm^{-3}. These are the typical ranges for very massive stars in their late evolution. Finally, plasmon decay and bremsstrahlung on nuclei are mostly important for large ($\rho \gtrsim 10^6$ g cm^{-3}) and extremely large ($\rho \gtrsim 10^9$ g cm^{-3}) core densities, respectively, and temperatures of the order of $10^8\,^\circ K \lesssim T \lesssim 10^{10}\,^\circ K$. Such conditions are typically realized in white dwarfs.

Starting from the first calculation of neutrino energy loss rates, based on the V-A theory of weak interactions [2,3], a systematic study of processes i)-iv) has been carried out in a long series of papers [2]-[22]. In all these analyses the pair production rate i) has been evaluated at order G_F^2, i.e. at the zero order in the electromagnetic coupling constant α expansion. Despite of the different topology and phase space volume which characterize the remaining processes ii)-iv), it is nevertheless worth noticing that they are instead at least of order αG_F^2. In view of this, it is therefore meaningful to investigate whether including QED radiative corrections to pair annihilation rate i) may lead to a sensible change in the cooling rate Q. This is the aim of this letter. In particular we report here the results of a calculation at order α of two classes of contributions, due to vacuum radiative corrections as well as those arising from the interaction of the e^+-e^- pairs with the surrounding electromagnetic plasma. This has been performed in the real time formalism for finite temperature field theory. We actually find that the total corrections to Q range in the interval $(-4 \div 1)\%$ of the tree level estimate, in the temperature and density ranges where the pair annihilation process represents the main contribution to the total energy loss rate. We have also re-evaluated both photoproduction and plasmon decay rates, and we do find a good agreement with the most

recent estimates reported in the literature [21,22].

The paper is organized as follows. Section 2 is a short review of the lowest order calculation of Q for the pair annihilation process. The order α QED corrections are then considered in Section 3, where we report the main results of our calculations of both *vacuum* and *thermal* contributions. We finally discuss our results and give our conclusions in Section 4.

2 Pair annihilation in Born approximation

We first consider the pair annihilation process $e^+ + e^- \to \nu + \overline{\nu}$ at the lowest order in perturbation theory. Denoting with $p_{1,2} \equiv (E_{1,2}, \vec{p}_{1,2})$, the energy-momentum of ingoing electron and positron, and with $q_{1,2} \equiv (\omega_{1,2}, \vec{q}_{1,2})$ the four-momentum of the outgoing neutrino and antineutrino, respectively, the neutrino energy loss rate Q is given by [1]

$$Q = \frac{1}{(2\pi)^6} \int \frac{d^3\vec{p}_1}{2E_1} \int \frac{d^3\vec{p}_2}{2E_2} \, (E_1 + E_2) \, F_-(E_1) \, F_+(E_2) \\ \times \left\{ \frac{1}{(2\pi)^2} \int \frac{d^3\vec{q}_1}{2\omega_1} \int \frac{d^3\vec{q}_2}{2\omega_2} \, \delta^4(p_1 + p_2 - q_1 - q_2) \sum_{\lambda,\beta} \left| M_{e^+e^- \to \nu_\beta \overline{\nu}_\beta} \right|^2 \right\} \ , \quad (1)$$

where $F_\pm(E) = \left[\exp\left\{ \frac{E}{T} \pm \xi_e \right\} + 1 \right]^{-1}$ are the Fermi-Dirac distribution functions for positrons/electrons with temperature T and degeneracy parameter ξ_e. Finally $\sum_{\lambda,\beta} \left| M_{e^+e^- \to \nu_\beta \overline{\nu}_\beta} \right|^2$ is the squared modulus of the reaction amplitude summed over all particle polarizations λ and neutrino flavours β.

In the Born approximation, i.e. in the limit of a four fermion electroweak interaction and no electromagnetic radiative corrections (see Fig. 1a), the quantity in curly brackets in Eq. (1) takes the form

$$\frac{2G_F^2}{3\pi} \left[\left(C_V'^2 + C_A'^2 \right) \left(m_e^2 + 2p_1 \cdot p_2 \right) + 3 \left(C_V'^2 - C_A'^2 \right) m_e^2 \right] (p_1 + p_2)^2 \ , \quad (2)$$

where we have defined $C_{V,A}'^2 \equiv (1 + C_{V,A})^2 + 2C_{V,A}^2$ with $C_V = 2\sin^2\theta_W - 1/2$, $C_A = -1/2$.

Substituting Eq. (2) into Eq. (1) and performing the angular integrations, we get the final expression for the energy loss rate induced by pair annihilation in the Born approximation,

[1] We use natural units, $\hbar = c = k = 1$.

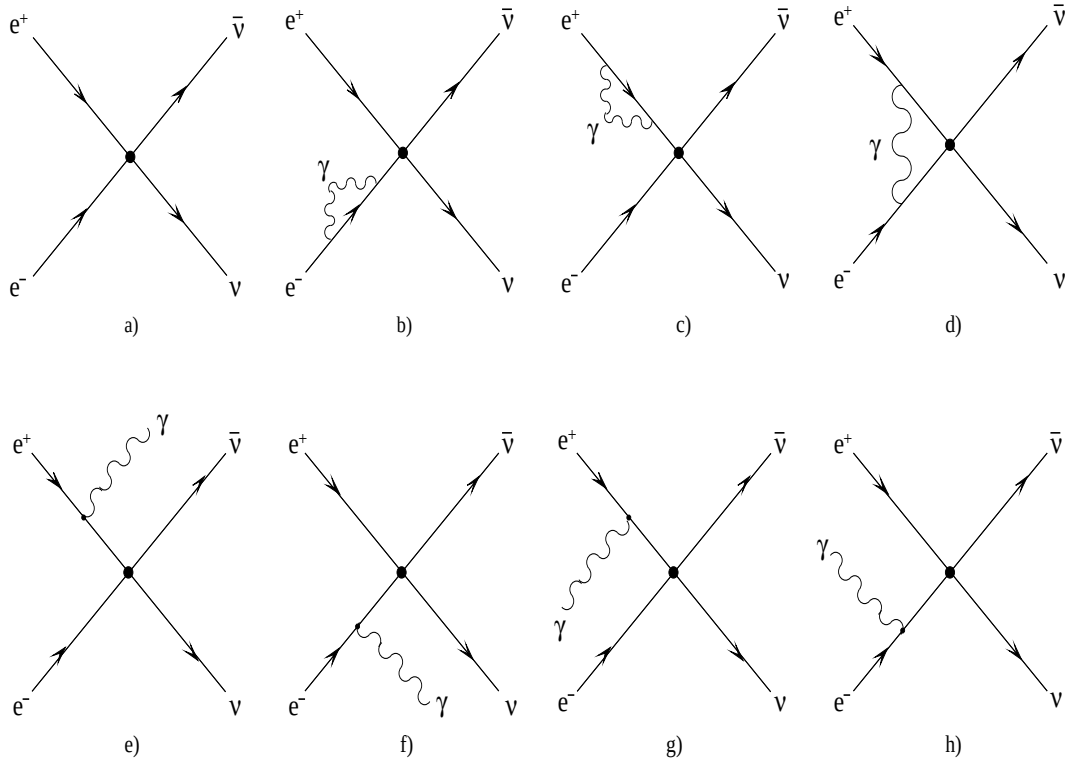

Fig. 1. Feynman diagrams for the pair annihilation process up to order αG_F^2.

$$Q_B = \frac{G_F^2\, m_e^4}{18\pi^5} \int_0^\infty \frac{|\vec{p}_1|^2\, d|\vec{p}_1|}{E_1} \int_0^\infty \frac{|\vec{p}_2|^2\, d|\vec{p}_2|}{E_2}\ (E_1+E_2)\, F_-(E_1) F_+(E_2)$$
$$\times\ \left[C_V'^2 \left(7 + 9\frac{E_1 E_2}{m_e^2} - \frac{E_1^2+E_2^2}{m_e^2} + 4\frac{E_1^2 E_2^2}{m_e^4} \right) \right.$$
$$\left. +\ C_A'^2 \left(-4 - \frac{E_1^2+E_2^2}{m_e^2} + 4\frac{E_1^2 E_2^2}{m_e^4} \right) \right] . \qquad (3)$$

Note that Q_B depends on the temperature T and the electron degeneracy parameter ξ_e only. It is customary to express the dependence on ξ_e (or the electron chemical potential) in terms of the matter density, ρ, the electron molecular weight, μ_e, and T through the condition of plasma electrical neutrality,

$$\frac{\rho}{\mu_e} = \frac{1}{\pi^2 N_A} \int_{m_e}^\infty E\sqrt{E^2 - m_e^2}\, dE\ \left(\frac{1}{\exp\left\{\frac{E}{T} - \xi_e\right\} + 1} - \frac{1}{\exp\left\{\frac{E}{T} + \xi_e\right\} + 1} \right) \quad , \qquad (4)$$

N_A being the Avogadro number.

In Fig. 2 we show the energy loss rate due to pair annihilation in the Born approximation for several values of the temperature as function of ρ/μ_e.

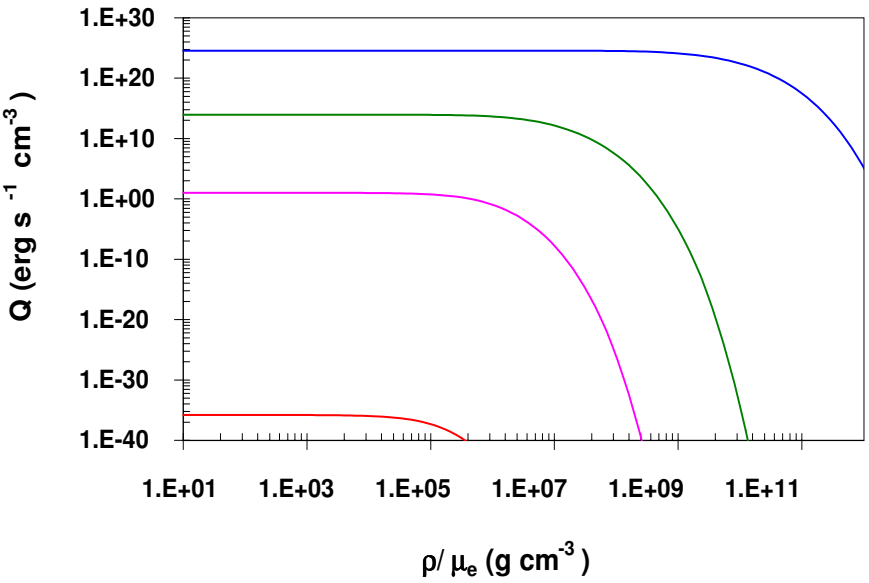

Fig. 2. The energy loss rate due to pair annihilation process in the Born approximation for $T = 10^8, 10^{8.5}, 10^9, 10^{10}\ ^\circ K$ (from bottom to top).

3 Pair annihilation: radiative corrections

A consistent computation up to order α of the energy loss rate Q due to pair annihilation is obtained by considering the additional contribution of all diagrams shown in Fig.s 1b-1h. Notice that since the energy carried by the outgoing neutrino pair is typically smaller or, at most, of the order of 1 MeV, we can safely neglect the electroweak radiative corrections to the four fermion effective interactions, and only consider the set of gauge invariant purely QED contributions.

The radiative corrections in case of large values of temperature and density must be computed taking into account the presence of the electromagnetic plasma, namely $e^\pm$ and γ. As long as neutrino mean free path is so large that they leave the star without any further interaction, there is no relevant neutrino component in the stellar plasma. The zero temperature radiative corrections, or *vacuum radiative corrections*, have been already computed in literature. They can be obtained for example, from the results of Ref. [23] by using crossing symmetry. It is customary to classify them as follows:

- electron mass and wavefunction renormalization (Fig.s 1b-1c);
- electromagnetic vertex correction (Fig. 1d);
- γ emission/absorption (Fig.s 1e-1h).

The whole radiative corrections, including the finite temperature effects, can be then obtained from the diagrams of Fig.s 1b-1h by using the real time

formalism for finite temperature quantum field theory. In this framework the thermal propagators for electrons and photons read as follow

$$S_T(p) = (\not{p} + m)\Big\{\frac{i}{p^2 - m_e^2 + i\epsilon} - 2\pi\,\delta\left(p^2 - m_e^2\right)\left[F_-(|p_0|)\Theta(p_0) + F_+(|p_0|)\Theta(-p_0)\right]\Big\} \quad , \tag{5}$$

$$D_T^{\alpha\beta}(k) = -\left[\frac{i}{k^2 + i\epsilon} + 2\pi\,\delta\left(k^2\right) B(|k_0|)\right] g^{\alpha\beta} \quad , \tag{6}$$

where $\Theta(x)$ is the step function and $B(x)$ is the Bose distribution function. The first terms in Eq. (5) and (6) are the usual $T = 0$ Feynman propagators, while those depending on the temperature (and density) through the distribution functions describe the interactions with real particles of the thermal bath.

The calculation for the order αG_F^2 corrections to the Born approximation for the energy loss rate proceeds in close analogy with what has been described in Ref.s [24,25] for a very similar situation. In particular, the additional contributions to Q due to mass, wave function and vertex corrections come from the interference between diagrams of Fig.s 1b, 1c and 1d with the Born amplitude of Fig. 1a. In addition, the energy loss rates due to γ emission (absorption) $Q_{e(a)}$, are given by the sum of squared amplitudes of the processes of Fig.s 1e, 1f (1g, 1h),

$$Q_e = \frac{1}{(2\pi)^9}\int\frac{d^3\vec{p}_1}{2E_1}\int\frac{d^3\vec{p}_2}{2E_2}\int\frac{d^3\vec{k}}{2\omega}\,(E_1 + E_2 - \omega)F_-(E_1)\,F_+(E_2)\,(1 + B(\omega)) \times\left\{\frac{1}{(2\pi)^2}\int\frac{d^3\vec{q}_1}{2\omega_1}\int\frac{d^3\vec{q}_2}{2\omega_2}\,\delta^4(p_1 + p_2 - q_1 - q_2 - k)\sum_{\lambda,\beta}|M_{e^+e^-\to\nu_\beta\overline{\nu}_\beta\gamma}|^2\right\} , \tag{7}$$

$$Q_a = \frac{1}{(2\pi)^9}\int\frac{d^3\vec{p}_1}{2E_1}\int\frac{d^3\vec{p}_2}{2E_2}\int\frac{d^3\vec{k}}{2\omega}\,(E_1 + E_2 + \omega)F_-(E_1)\,F_+(E_2)\,B(\omega) \times\left\{\frac{1}{(2\pi)^2}\int\frac{d^3\vec{q}_1}{2\omega_1}\int\frac{d^3\vec{q}_2}{2\omega_2}\,\delta^4(p_1 + p_2 - q_1 - q_2 + k)\sum_{\lambda,\beta}|M_{e^+e^-\gamma\to\nu_\beta\overline{\nu}_\beta}|^2\right\} . \tag{8}$$

For the seek of brevity we do not report here the details of our calculation leaving this lengthy description to a forthcoming paper [26]. We only briefly outline the method adopted to obtain the final corrections ΔQ. Each of the several contribution to $|M_{e^+e^-\to\nu_\beta\overline{\nu}_\beta}|^2$, and the two squared amplitude $|M_{e^+e^-\to\nu_\beta\overline{\nu}_\beta\gamma}|^2$ and $|M_{e^+e^-\gamma\to\nu_\beta\overline{\nu}_\beta}|^2$ have been evaluated analytically. The results should be then integrated over the relevant phase space. Some of these integrations can be again done analytically, while we have used a Montecarlo technique to deal

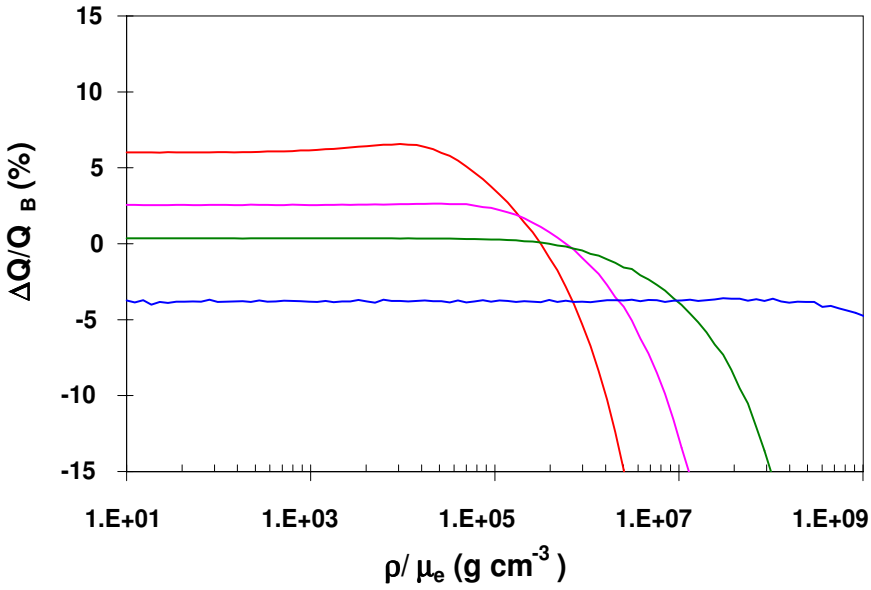

Fig. 3. The total radiative corrections normalized to the Born approximation result for the pair annihilation process for $T = 10^8, 10^{8.5}, 10^9, 10^{10}\ ^\circ K$ (from top to bottom).

with the (usually three of five-dimensional) remaining integrations, requiring an accuracy better than 1% on ΔQ [2]. The main difficulty of this procedure is that each contribution coming from the interference of diagrams 1b)-1d), as well as the squared amplitudes 1e)-1h) is plagued by infrared divergencies, while the overall result is of course divergence free. To regularize these divergencies we have explicitly subtracted all divergent terms expanding the squared amplitudes in a Laurent series around the pole singularities. This method follows quite closely what has been already used in [24,25,27].

In Fig. 3 we show the ratio between the sum of all radiative corrections and Q_B, $\Delta Q/Q_B$, for some values of T as a function of the density. For a fixed value of temperature, the ratio $\Delta Q/Q_B$, shows a plateau, for all densities for which the electron-positron chemical potential is smaller than the temperature, so that the mean energy is essentially given by T. The plateau end point, as expected, shifts towards larger values of ρ_{μ_e} with increasing temperature. For even larger densities the mean energy of the $e^+ - e^-$ pair is dominated by their Fermi energy ϵ_F, and the ratio $\Delta Q/Q_B$ start varying logarithmically as a function of ϵ_F/m_e. Similarly, at fixed density and increasing temperature,

[2] The accuracy is actually depending on the values of temperature and density. The estimate of 1% for the theoretical error is rather conservative, and represents the larger result in the whole interval where pair annihilation significantly contribute to the cooling rate Q, $10^9\,^\circ K \leq T \leq 10^{10}\,^\circ K$. For smaller values of T, since the pair annihilation process rate is very small, the accuracy gets worst, and in our calculations can reach 5%.

where the effect of degeneracy can be neglected, the ratio $\Delta Q/Q_B$ shows a similar logarithmic behaviour as function of T/m_e [3]. Both these behaviours suggest that in these extreme regimes higher order QED contributions should be included. However, the trends exhibited in Fig. 3 cannot be straightforwardly extrapolated where T or ϵ_F start to be closer to the W and Z masses, since the effects of electroweak corrections should be taken into account as well. Furthermore it is also worth noticing that for temperatures larger than $10^{10}\,^\circ K$, and/or densities larger than, say 10^{12} g cm^{-3}, the neutrino mean free path becomes of the order or smaller than the dimension of the star core, so that neutrinos start interacting with the medium. This means that to evaluate the cooling rate via neutrino emission it is necessary to consider their Pauli blocking factors, as well as the (negative) contribution due to inverse processes.

It is actually interesting to see how the increasing importance of radiative corrections with temperature and density in the range of interest emerges from the study of other parameters which characterise the properties of the electromagnetic plasma, like thermal effective masses of particles. In general, thermal masses would show an explicit dependence on the spatial momentum $\vec{p}$. Nevertheless a nice way to see how their dispersion relations are influenced by interactions is to consider their average over the equilibrium distribution. In particular, for the electron effective mass we have

$$< m_e^R >= \frac{1}{\pi^2\, n_-} \int_0^\infty |\vec{p}|^2\, d|\vec{p}|\; m_e^R(|\vec{p}|)\; F_-(E) \quad , \tag{9}$$

where n_- is the electron number density and $m_e^R(|\vec{p}|)$ is the momentum-dependent renormalized mass in the electromagnetic plasma with temperature T and density ρ/μ_e,

$$\begin{aligned} m_e^R(|\vec{p}|) = m_e + \frac{\alpha\pi}{3}\frac{T^2}{m_e} + \frac{\alpha}{\pi m_e}\int_0^\infty \frac{|\vec{k}|^2\, d|\vec{k}|}{\omega}\left(F_-(\omega)+F_+(\omega)\right) - \frac{\alpha m_e}{2\pi|\vec{p}|}\int_0^\infty \frac{|\vec{k}|\, d|\vec{k}|}{\omega} \\ \times\left(F_-(\omega)\log\left(\frac{\omega E - m_e^2 + |\vec{p}||\vec{k}|}{\omega E - m_e^2 - |\vec{p}||\vec{k}|}\right) - F_+(\omega)\log\left(\frac{\omega E + m_e^2 + |\vec{p}||\vec{k}|}{\omega E + m_e^2 - |\vec{p}||\vec{k}|}\right)\right), \end{aligned} \tag{10}$$

where $\omega = \sqrt{|\vec{k}|^2 + m_e^2}$. An analogous result for positron can be obtained from (10) with the substitutions $F_\pm(\omega) \to F_\mp(\omega)$.

[3] See, for example, the typical behaviour of QED radiative corrections for a similar process in [23]

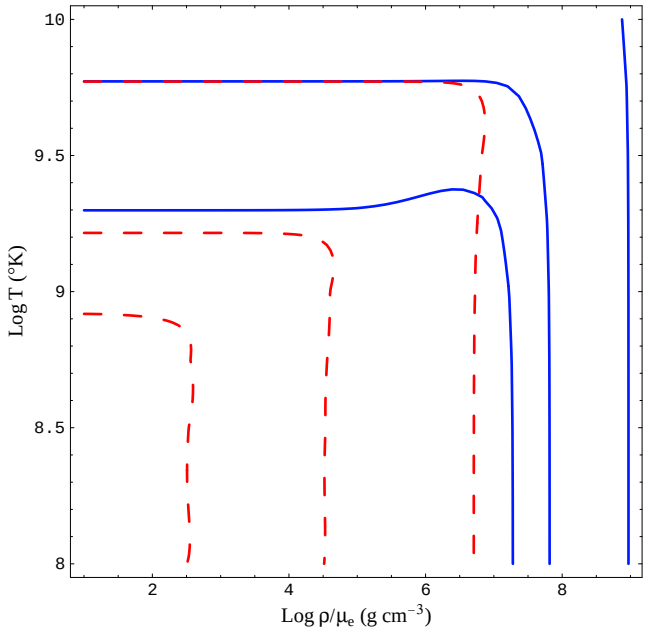

Fig. 4. Contour plots for the photon (dashed lines) and the electron (solid lines) thermal mass correction, normalized to m_e. The electron effective mass has been averaged over the thermal equilibrium distribution. From left to right the curves refer to the values 10^{-3}, 10^{-2}, and 10^{-1}.

For the photon thermal mass the averaging is unnecessary, since it does not depend on the spatial momentum

$$m_\gamma^2 = \frac{4\alpha}{\pi} \int_0^\infty \frac{|\vec{k}|^2 \, d|\vec{k}|}{\omega} \left(F_-(\omega) + F_+(\omega) \right) \quad . \tag{11}$$

In Fig. 4 we have reported the contour plots of $(< m_e^R > - m_e)/m_e$ and m_γ/m_e in the temperature-density plane. Curves from left to right refer to the values 10^{-3}, 10^{-2} and 10^{-1}, respectively. From this plot it is clear that both electron and photon effective masses grows logarithmically with the particle mean energy, and are again of the order of few percent in the relevant range of temperature and density.

4 Results and conclusions

In this letter we have reported on the calculation of the energy loss rate of pair annihilation process i) up to order αG_F^2. The Born value for Q has been corrected including both *vacuum* and *thermal* radiative corrections, the latter being computed in the real time formalism. One of our main results is presented in Fig. 3, where we plot these radiative corrections with respect to

the Born approximation estimate, as functions of the plasma density for some values of the temperature. The corrections come out to be of the order of few percent and negative for high temperatures, implying that for these temperatures the energy loss is sensibly decreased. At fixed temperature, $\Delta Q/Q_B$ goes to a constant value for low density. This can be easily understood, since in this limit the plasma is weakly degenerate, and therefore the energy loss rate depends on temperature only. At large densities the ratio $\Delta Q/Q_B$ decreases and reach larger negative values. However for such high densities the pair annihilation rates are exceedingly small and thus this process gives only a marginal contribution to the star cooling.

In order to perform a comprehensive study of order αG_F^2 contributions to the energy loss rate, we have also recalculated the contribution from ν-photoproduction and plasmon decay processes. While the detailed analytical calculations will be discussed elsewhere [26], we here give our numerical results in Fig. 5, where we show the several contributions to Q. When possible, we also show for comparison the results of Ref. [22]. In particular our results for these processes agree quite nicely, at least in the whole region where they significantly contribute to the total energy loss rate. For the bremsstrahlung on nuclei we have used the analytic fitting formula of Ref. [22].

Fig. 5 shows that, as well known, for large temperatures and not too high densities, pair annihilation dominates over the other two processes, while for low densities ν-photoproduction dominates over plasmon decay. On the other hand, for large densities the most relevant process is plasmon decay, whose rate however, along with those of all other processes, rapidly falls down for extremely high densities. This is a genuine plasma effect. Consider, for example, the behaviour of ν-photoproduction energy loss. As already noted in [3], the decrease for very large densities is achieved only if one consistently takes into account the increasingly large photon thermal mass. In fact with a massless photon the ν-photoproduction curves in Fig. 5 would rather reach a constant value. The main effect of m_γ^2 is a lowering of the values of the Bose distribution function for photons, i.e. a smaller number of thermal photons. This reduces the energy loss rate induced by ν-photoproduction.

In Fig. 6 we show the regions in the temperature-density plane where a given process contributes to the total energy loss rate (including radiative corrections to pair annihilation) for more than 90%. We also summarize there our results on the radiative corrections to pair annihilation processes, by plotting the contours corresponding to $\Delta Q/Q^0_{Tot} = 1\%, 0\%, -1\%, -2\%, -3\%, -4\%$, where Q^0_{Tot} is the total emission rate with pair annihilation calculated in Born approximation. These contours lie almost entirely in the region where the pair annihilation process gives the main contribution to Q. This result may affect the late stages of evolution of very massive stars by changing their configuration at the onset of Supernova explosion. This issue is presently under study.

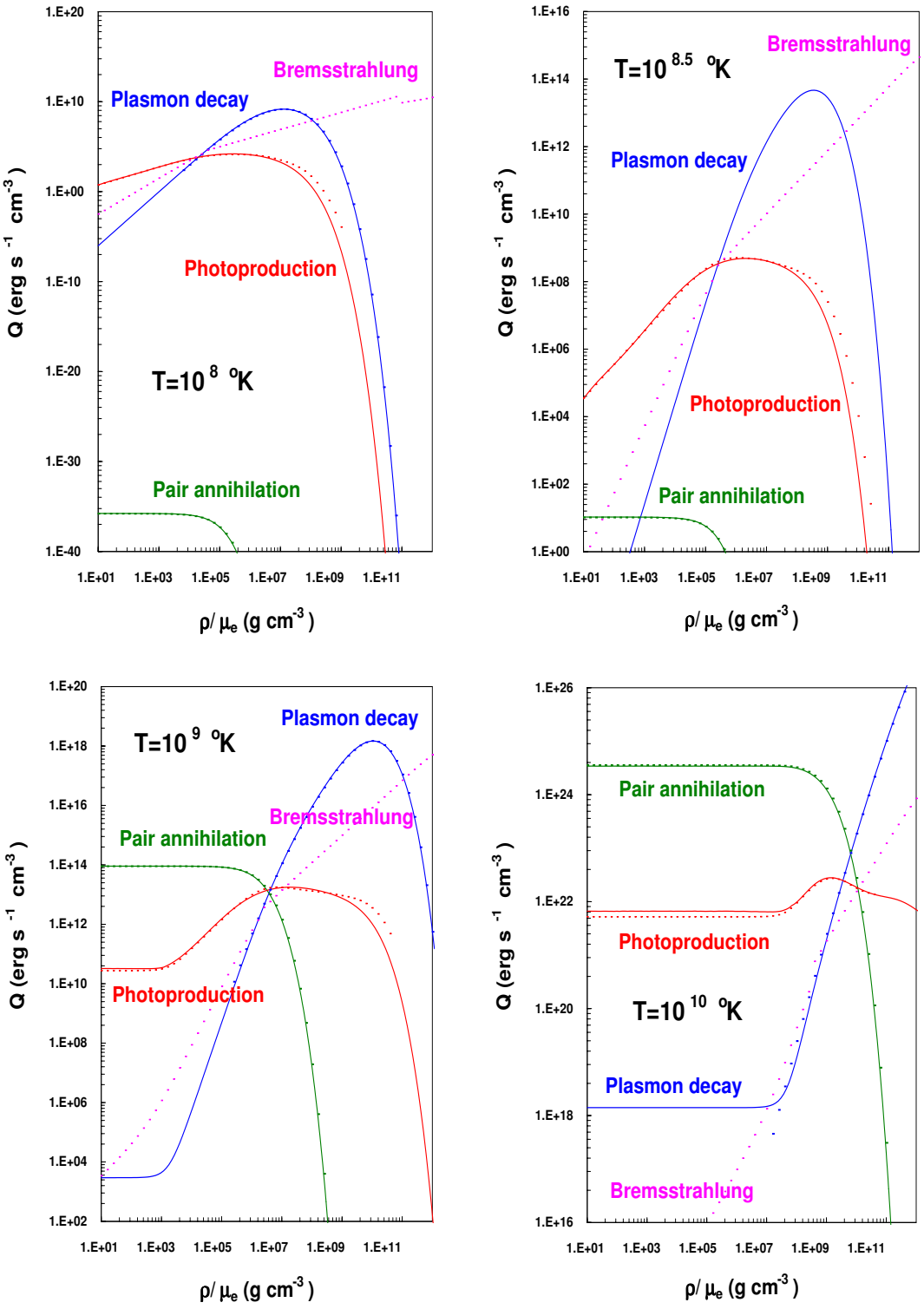

Fig. 5. The energy loss rate versus ρ/μ_e due to pair annihilation (including radiative corrections), photoproduction and plasmon decay (solid lines) for several temperatures. The dotted lines refer to the analogous results of Ref. [22], which also compute the rate for bremsstrahlung on nuclei. The effect of ΔQ to pair annihilation can be appreciated in this logarithmic scale only for the largest temperature $10^{10}\,^{\circ}K$.

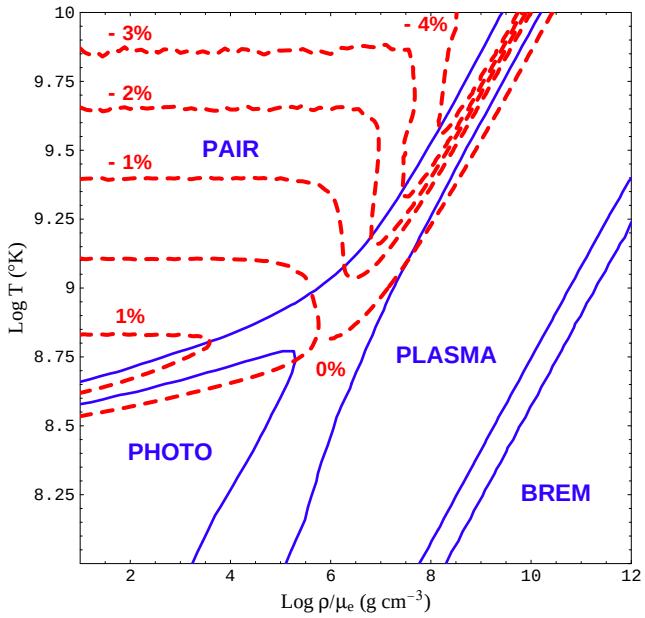

Fig. 6. The regions in the $T-\rho/\mu_e$ plane where each of the processes i)-iv) contribute for more than 90% to the total energy loss rate. We also show the contours for the relative correction $\Delta Q/Q^0_{Tot}$ (see text) for the values $1\%, 0\%, -1\%, -2\%, -3\%, -4\%$.

5 Acknowledgements

We warmly thank M. Passera for a clarifying correspondence and suggestions. We are also pleased to thank A. Chieffi, G.Imbriani, M. Limongi, L. Piersanti and O. Straniero for useful discussions.

References

[1] see for example H.T. Janka, K. Kifonidis, and M. Rampp, Proc. of *ECT International Workshop on Physics of Neutron Star Interiors*, Ed.s D. Blaschke, N.K. Glendenning, and A.D. Sedrakain, Springer; astro-ph/0103015.

[2] V. Petrosian, G. Beaudet, and E.E. Salpeter, *Phys. Rev.* **154** (1967) 1445.

[3] G. Beaudet, V. Petrosian, and E.E. Salpeter, *Ap.J.* **150** (1967) 979.

[4] D.A. Dicus, *Phys.Rev.* **D6** (1972) 941.

[5] D.A. Dicus, E.W. Kolb, D.N. Schramm, and D.L. Tubbs, *Ap.J.* **210** (1976) 481.

[6] N. Itoh and Y. Kohyama, *Ap.J.* **275** (1983) 858.

[7] N. Itoh, N. Matsumoto, M. Seki, and Y. Kohyama, *Ap.J.* **279** (1984) 413.

[8] N. Itoh, Y. Kohyama, N. Matsumoto, and M. Seki, *Ap.J.* **280** (1984) 787; erratum, **404** (1993) 418.

[9] N. Itoh, Y. Kohyama, N. Matsumoto, and M. Seki, *Ap.J.* **285** (1984) 304; erratum, **322** (1987) 584.

[10] H. Munakata, Y. Kohyama, and N. Itoh, *Ap.J.* **296** (1985) 197; erratum, **304** (1986) 580.

[11] Y. Kohyama, N. Itoh, and H. Munakata, *Ap.J.* **310** (1986) 815.

[12] H. Munakata, Y. Kohyama, and N. Itoh, *Ap.J.* **316** (1987) 708.

[13] P.J. Schinder, D.N. Schramm, P.J. Wiita, S.H. Margolis, and D.L. Tubbs, *Ap.J.* **313** (1987) 531.

[14] N. Itoh, T. Adachi, M. Nakagawa, Y. Kohyama, and H. Munakata, *Ap.J.* **339** (1989) 354; erratum, **360** (1990) 741.

[15] N. Itoh, K. Kojo, and M. Nakagawa, *Ap.J. Suppl.* **74** (1990) 291.

[16] E. Braaten, *Phys.Rev.Lett.* **66** (1991) 1655.

[17] N. Itoh, H. Mutoh, A. Hikita, and Y. Kohyama, *Ap.J.* **395** (1992) 622; erratum, **404** (1993) 418.

[18] Y. Kohyama, N. Itoh, A. Obama, and H. Mutoh, *Ap.J.* **415** (1993) 267.

[19] E. Braaten and D. Segel, *Phys.Rev.* **D48** (1993) 1478.

[20] Y. Kohyama, N. Itoh, A. Obama, and H. Hayashi, *Ap.J.* **431** (1994) 761.

[21] M. Haft, G. Raffelt, and A. Weiss, *Ap.J.* **425** (1994) 222; erratum, **438** (1995) 1017.

[22] N. Itoh, H. Hayashi, A. Nishikawa, and Y. Kohyama, *Ap.J.S.* **102** (1996) 411.

[23] M. Passera, *Phys.Rev.* **D64** (2001) 113002.

[24] S. Esposito, G. Mangano, G. Miele, and O. Pisanti, *Phys.Rev.* **D8** (1998) 105023.

[25] S. Esposito, G. Mangano, G. Miele, and O. Pisanti, *Nucl.Phys.* **B540** (1999) 3.

[26] S. Esposito, G. Mangano, G. Miele, I. Picardi, and O. Pisanti, in preparation.

[27] J.L Cambier, J.R.Primack, and M. Sher, *Nucl. Phys.* **B209** (1982) 372.